
RoMA: a Method for Neural Network Robustness Measurement and Assessment

Natan Levy^{1*} Guy Katz^{1*}

Abstract

Neural network models have become the leading solution for a large variety of tasks, such as classification, language processing, and others. However, their reliability is heavily plagued by *adversarial inputs*: inputs generated by adding tiny perturbations to correctly-classified inputs, and for which the neural network produces erroneous results. In this paper, we present a new method called *Robustness Measurement and Assessment (RoMA)*, which measures the robustness of a neural network model against such adversarial inputs. Specifically, RoMA determines the probability that a random input perturbation might cause misclassification. The method allows us to provide formal guarantees regarding the expected frequency of errors that a trained model will encounter after deployment. The type of robustness assessment afforded by RoMA is inspired by state-of-the-art certification practices, and could constitute an important step towards integrating neural networks in safety-critical systems.

1. INTRODUCTION

In the passing decade, deep neural networks (DNNs) have emerged as one of the most exciting developments in computer science, allowing computers to outperform humans in various classification tasks. However, a major issue with DNNs is the existence of *adversarial inputs* (Goodfellow et al., 2014): inputs that are very close (according to some metrics) to correctly-classified inputs, but which are misclassified themselves. It has been observed that many state-of-the-art DNNs are highly vulnerable to adversarial inputs (Carlini & Wagner, 2017), and it has been suggested that adversarial inputs are an inescapable part of the neural network architecture (Ilyas et al., 2019).

As the impact of the AI revolution is becoming evident, regulatory agencies are starting to address the challenge of integrating DNNs into various automotive and aerospace systems — by forming workgroups to create the needed guidelines. Notable examples in the European Union include SAE G-34 and EUROCAE WG-114 (Pereira & Thomas, 2020; Vidot et al., 2021); and the European Union Safety Agency (EASA), which is responsible for civil aviation safety, and which has published a road map for certifying AI-based systems (European Union Aviation Safety Agency, 2020). These efforts, however, must overcome a significant gap: on one hand, the superior performance of DNNs makes it highly desirable to incorporate them into various systems, but on the other hand, the DNN’s intrinsic susceptibility to adversarial inputs could render them unsafe. This dilemma is particularly felt in safety-critical systems, such as automotive, aerospace and medical devices, where regulators and public opinion set a high bar for reliability (Dmitriev et al., 2021).

In this work, we seek to begin bridging this gap, by devising a framework that could allow engineers to *bound and mitigate* the risk introduced by a DNN, effectively containing the phenomenon of adversarial inputs. Our approach is inspired by common practices of regulatory agencies, which often need to certify various systems with components that might fail due to an unexpected hazard. A widely used example is the certification of jet engines, which are known to occasionally fail. In order to mitigate this risk, manufacturers compute the engines’ *mean time between failures (MTBF)*, and then use this value in performing a *functional hazard analysis (FHA)* — which can eventually justify the safety of the jet engine system as a whole (FAA, 2021a). For example, the *Federal Aviation Administration (FAA)* guides that the probability for a catastrophic failure event per operational hour should not exceed 10^{-9} (FAA, 2021b). To perform a similar process for DNN-based systems, we first need a technique for accurately bounding the likelihood of a failure to occur — e.g., for measuring the probability of encountering an adversarial input.

In this paper, we address the aforesaid crucial gap by introducing a straightforward and scalable method for measuring the probability that a DNN classifier misclassifies inputs. The method, which we term *Robustness Measurement and*

^{*}Equal contribution ¹Department of Computer Science and Engineering, Hebrew University, Jerusalem, Israel. Correspondence to: Natan Levy <natan.levy1@mail.huji.ac.il>, Guy Katz <guykatz@cs.huji.ac.il>.

Assessment (RoMA), is inspired by modern certification concepts, and operates under the assumption that a DNN’s misclassification is due to some internal malfunction, caused by random input perturbations (as opposed to misclassifications triggered by an external cause, such as a malicious adversary). A random input perturbation can occur naturally as part of the system’s operation, e.g., due to scratches on a camera lens or communication disruptions. Under this assumption, RoMA can be used to measure the model’s robustness to randomly-produced adversarial inputs. The proposed method has several applications, such as comparing the robustness of multiple models and picking the best one; checking the impact of various configurable parameters (e.g., the number of training epochs, or the magnitude of the input perturbation) on the model’s robustness; or as part of a functional hazard analysis, as previously described.

RoMA is a method for estimating rare events in a large population — in our case, adversarial inputs within a space of inputs that are generally classified correctly. The method relies on the properties of *normal distributions*. Intuitively, if it is known that the rare events (adversarial inputs) are distributed normally within the input space, it is usually sufficient to: sample a few hundred random input points; measure the “level of adversariality” of each such point; use these measurements to draw a Gaussian curve; and then use the normal distribution function to evaluate the probability of encountering an adversarial input within the input space. Unfortunately, adversarial inputs are often not distributed normally. To overcome this difficulty, RoMA first applies a *power transformation* called Box-Cox (Box & Cox, 1982), after which the distribution often becomes normal and can be analyzed.

At a high level, RoMA consists of the following steps:

1. for an arbitrary input point from the test set \vec{x}_0 , we randomly sample n perturbations of \vec{x}_0 (usually, a few hundreds), and obtain a set of perturbed inputs $\{\vec{x}^1, \dots, \vec{x}^n\}$;
2. we evaluate the DNN on each \vec{x}^i , obtaining the corresponding outputs $\{\vec{y}_0^1, \dots, \vec{y}_0^n\}$;
3. for each \vec{y}_0^i , we collect the maximal entry in \vec{y}_0^i assigned to any label other than the correct label (that is, other than to the original label assigned to \vec{x}_0 by the data set). These values, which we term the *highest incorrect confidence (hic)* scores, represent how close each \vec{x}^i is to being an adversarial input;
4. if the hic score data does not distribute normally (according to the Anderson-Darlin goodness-of-fit test (Anderson, 2011)), we apply a power transformation called Box-Cox (Box & Cox, 1982) to normalize its distribution; and

5. if the distribution is now normal, we use the properties of the normal distribution function to calculate the probability for an adversarial input around \vec{x}_0 .

The Box-Cox statistical power transformation, which RoMA uses for normalizing the distribution of confidence scores assigned to incorrect labels, is a widespread method that does not pose any restrictions on the DNN in question (e.g., Lipschitz continuity, certain kinds of activation functions, or specific network topology). Further, the method does not require access to the network’s design or weights, and is thus applicable to large, black-box DNNs.

We implemented our method as a proof-of-concept tool, and evaluated it on standard DNN architectures: VGG16 (Simonyan & Zisserman, 2015), Resnet (He et al., 2016), and Densenet (Huang et al., 2017a), all trained on the CIFAR10 data set (Krizhevsky & Hinton, 2009). We used RoMA to compare the robustness of these DNN models and found, as expected, that a higher number of epochs (i.e., high level of training) leads to a higher robustness score. Additionally, we used RoMA to measure how the allowed magnitude of perturbation affects the robustness of a DNN model. Finally, using RoMA, we found that the *categorical robustness* score of a DNN (i.e., the robustness score of inputs labeled as a particular category) *varies significantly* among the different categories. This finding could allow users and regulators to specify different acceptable robustness thresholds for each target category, instead of a single global threshold, which may not fit the entire system. The concept of measuring the robustness score per category is in line with aerospace software certification guidelines (DO-178), where different sub-systems often require different *design assurance levels (DALs)* (Federal Aviation Administration, 1993).

To summarize, our main contributions are:

- Introducing RoMA: a new method for measuring the robustness of a DNN model. The new method is scalable and can run on black-box DNNs.
- Comparing the robustness of multiple state-of-the-art DNN models.
- Using RoMA to measure the effect of perturbation level has on the robustness of the DNN model.
- Formally computing *categorical robustness* scores, and demonstrating that they can differ significantly between labels.

Related work. The topic of evaluating a model’s adversarial robustness has been studied extensively. Some notable approaches include:

- Statistical approaches that evaluate the probability of encountering an adversarial input in the population. In

recent papers (Huang et al., 2021; Cohen et al., 2019), Huang et al. and Cohen et al. use random sampling, which is similar in spirit to RoMA, but which assumes that the perturbed images’ scores are distributed normally — and as we later demonstrate, this assumption often does not hold. In another paper, Webb et al. (Webb et al., 2018) use a sampling method called *multi-level splitting*, which provides no formal guarantee of the DNN’s robustness. Mangal et al. (Mangal et al., 2019) use *importance sampling*, which might be biased due to lack of sampling in areas of the population that are deemed *unimportant*. Moreover, Mangal’s approach assumes that the network’s output is Lipschitz-continuous, which limits its applicability. In contrast, RoMA requires no Lipschitz-continuity assumptions, does not assume a-priori that the adversarial inputs are distributed normally, and provides rigorous robustness guarantees.

- Formal-verification based approaches (Katz et al., 2017; Wang et al., 2018; Jacoby et al., 2020; Wu et al., 2020; Amir et al., 2021; Katz et al., 2021), which allow for computing a DNN’s exact adversarial robustness score. These approaches typically convert the problem into a constraint satisfiability problem, and then apply search and deduction procedures to solve it efficiently. However, verification-based approaches afford only limited scalability, and operate strictly on white-box DNNs. In contrast, RoMA is a scalable technique, and can operate on black-box DNNs.
- Approaches for computing an estimate bound on the probability that a classifier’s margin function exceeds a given value (Weng et al., 2019; Anderson & Sojoudi, 2020; Dvijotham et al., 2018). These analyses focus on the worst-case behavior, thus producing bounds that might be inadequate for regulatory certification. In contrast, RoMA focuses on the average case, which is more realistic in many application domains.

Outline. We begin with some needed background on adversarial robustness in Section 2. We then describe our proposed method for measuring adversarial robustness in Section 3, followed by a description of our evaluation setup in Section 4. In Section 5 we summarize and discuss our results.

2. Background

Neural Network. A neural network N is a function $N : \mathbb{R}^n \rightarrow \mathbb{R}^m$, which maps a real-valued input vector $\vec{x} \in \mathbb{R}^n$ to a real-value output vector $\vec{y} \in \mathbb{R}^m$. For classification networks, which is our subject matter, \vec{x} is classified as label l if y ’s l ’th entry has the highest score; i.e., if $\arg \max(N(\vec{x})) = l$.

Local Adversarial Robustness. The local adversarial robustness of a DNN is a measure of how resilient that network is against adversarial perturbations to specific inputs. Intuitively, a network with high robustness behaves “smoothly”, i.e., small perturbations to its input do not cause significant spikes in its output. More formally (Bastani et al., 2016; Huang et al., 2017b):

Definition 2.1. A DNN N is ϵ -locally-robust at input point \vec{x}_0 iff

$$\forall \vec{x}. \|\vec{x} - \vec{x}_0\|_\infty \leq \epsilon \Rightarrow \arg \max(N(\vec{x})) = \arg \max(N(\vec{x}_0))$$

Intuitively, Definition 2.1 states that for input vector \vec{x} , which is at a distance at most ϵ from a fixed input \vec{x}_0 , the network function assigns to \vec{x} the same label that it assigns to \vec{x}_0 (for simplicity, we use here the L_∞ norm, but other metrics could also be used). When a network is *not* ϵ -local-robust at point \vec{x}_0 , there exists a point \vec{x} that is at a distance of at most ϵ from \vec{x}_0 , which is misclassified; this \vec{x} is called an *adversarial input*. In this context, *local* refers to the fact that \vec{x}_0 is fixed. Larger values of ϵ imply a larger distance from \vec{x}_0 , and hence a stronger robustness guarantee if the property holds. Intuitively, in a DNN for image classification that is ϵ -local-robust, small perturbations to \vec{x}_0 , (i.e., tiny perturbations that a human would fail to detect), should not result in a change of predicted class.

Distinct Adversarial Robustness. Recall that the label assigned by a classification network is selected according to its greatest output value. The final layer in such networks is often a softmax layer, and its outputs are commonly interpreted as confidence scores assigned to each of the possible labels.¹ We use $c(\vec{x})$ to denote the highest confidence score, i.e. $c(\vec{x}) = \max(N(\vec{x}))$.

We are interested in an adversarial input \vec{x} only if it is *distinctly* misclassified, i.e., if \vec{x} ’s assigned label receives a significantly higher confidence score than that of the label assigned to \vec{x}_0 . For example, if $\arg \max(N(\vec{x}_0)) \neq \arg \max(N(\vec{x}))$, but the corresponding confidence score is $c(\vec{x}) = 0.4$, then \vec{x} is not distinctly an adversarial input: it is misclassified, but the network is not confident about this misclassification. In contrast, a case where $c(\vec{x}) = 0.8$ is clearly much more relevant. We refer to adversarial inputs which are misclassified with high confidence (greater than some threshold δ) as *distinctly adversarial inputs*, and refine Definition 2.1 to only consider them, as follows:

Definition 2.2. A DNN N is (ϵ, δ) -distinctly-locally-robust at input point \vec{x}_0 , iff

$$\forall \vec{x}. \|\vec{x} - \vec{x}_0\|_\infty \leq \epsilon \Rightarrow (\arg \max(N(\vec{x})) = \arg \max(N(\vec{x}_0)) \vee (c(\vec{x}) < \delta))$$

¹The term *confidence* is sometimes used to represent the reliability of the DNN as a whole; this is not our intention here.

Intuitively, if the definition does not hold then there exists a (distinctly) adversarial input \vec{x} that is at most ϵ away from \vec{x}_0 , and which is assigned a label different than that of \vec{x}_0 with a confidence score that is at least δ .

3. The Proposed Method

3.1. Probabilistic Robustness

Definitions 2.1 and 2.2 are geared for an external, malicious adversary: they are concerned with the existence of an adversarial input, implicitly assuming the adversary will be successful in finding it if such an input exists. Here, we follow common certification methodologies that deal with internal malfunctions of the system (Federal Aviation Administration, 1993), and focus on non-malicious adversaries. Differently put, we assume that perturbations occur naturally, and are not necessarily malicious — and this is represented by assuming that perturbations are generated *randomly*. We argue that the non-malicious adversary setting is more realistic for widely-deployed systems, such as medical devices, aerospace, and trains, which are expected to operate at a large scale for a prolonged period, and are more likely to randomly encounter adversarial inputs than those crafted by a malicious adversary.

Targeting randomly generated adversarial inputs requires extending Definitions 2.1 and 2.2 into a probabilistic definition, as follows:

Definition 3.1. The (δ, ϵ) -probabilistic-local-robustness score of a DNN N at input point \vec{x}_0 , abbreviated $\text{plr}_{\delta, \epsilon}(N, \vec{x}_0)$, is defined as:

$$\text{plr}_{\delta, \epsilon}(N, \vec{x}_0) \triangleq P_{x: \|\vec{x} - \vec{x}_0\|_{\infty} \leq \epsilon} [(\arg \max(N(\vec{x})) = \arg \max(N(\vec{x}_0)) \vee c(\vec{x}) < \delta)]$$

Intuitively, the definition measures the probability that an input \vec{x} , drawn at random from the ϵ -ball around \vec{x}_0 , will either have the same label as \vec{x}_0 or, if it does not, will receive a confidence score lower than δ for its (incorrect) label.

A key point is that probabilistic robustness, as defined in Definition 3.1 is a scalar value: the closer this value is to 1, the less likely it is a random perturbation to \vec{x}_0 would produce a distinctly adversarial input. This is in contrast to Definitions 2.1 and 2.2, which are Boolean in nature. We also note that the probability value in Definition 3.1 can be computed with respect to values of \vec{x} drawn according to any input distribution of interest. For simplicity, unless otherwise stated, we assume that \vec{x} is drawn uniformly at random.

In practice, we propose to compute $\text{plr}_{\delta, \epsilon}(N, \vec{x})$ by first computing the probability that a randomly drawn \vec{x} is an

adversarial input, and then taking that probability’s complement. Unfortunately, directly bounding the probability of randomly encountering an adversarial input, e.g., with the Monte Carlo or Bernoulli methods (Hammersley, 2013), is not feasible due to the typical extreme sparsity of adversarial inputs, and the large number of samples required to achieve reasonable accuracy (Webb et al., 2018). Thus, we require a different statistical approach to obtain this measure, using only a small number of samples. We next propose such an approach.

3.2. Sampling Method and the Normal Distribution

Our approach is to measure the probability of randomly encountering an adversarial input, by examining a finite set of perturbed samples around \vec{x}_0 . Each perturbation is selected through *simple random sampling* (Taherdoost, 2016), so that the overall perturbation size to the input features of \vec{x}_0 does not exceed the given ϵ . Next, each perturbed input \vec{x} is passed through the DNN to obtain a vector of confidence scores for the possible output labels. From this vector, we extract the *highest incorrect confidence (hic)* score

$$\text{hic}(\vec{x}) = \max_{i \neq \arg \max(N(\vec{x}_0))} \{N(\vec{x})[i]\}$$

which is the highest confidence score assigned to an *incorrect* label, i.e., a label different from the one assigned to \vec{x}_0 . Observe that input \vec{x} is distinctly adversarial if and only if its hic score exceeds the δ distinctness threshold (assuming $\delta > 0.5$), and so hic values can serve as a proxy for deciding the “adversarially” of \vec{x}_0 .

The main remaining question is how to extrapolate from the collected hic values a conclusion regarding the hic values in the general population. The normal distribution is a useful notion in this context: if the hic values are distributed normally (as determined by a statistical test), it is straightforward to obtain such a conclusion, even if adversarial inputs are scarce.

To illustrate this process, we trained a VGG16-10 DNN model (information about the trained model and the dataset appears in Section 4), and examined an arbitrary point \vec{x}_0 , classified as some label l_0 , from its training set. We randomly generated 10,000 perturbed images from \vec{x}_0 with $\epsilon = 0.04$, and ran them through the DNN. For each output vector obtained this way we collected the hic value, and then plotted these values as the blue histogram in Figure 1. The green curve represents the normal distribution using the average and standard deviation of the raw data. As the figure shows, the data is normally distributed; this claim is supported by running a “goodness-of-fit” test (explained later).

Our goal is to compute the probability of a fresh, randomly-perturbed input to be misclassified, i.e. to be assigned a

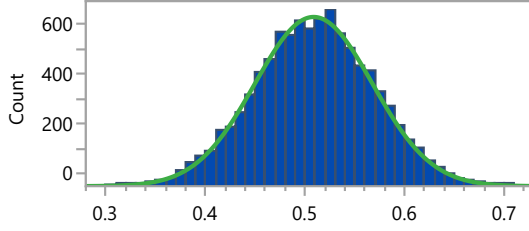


Figure 1. A histogram depicting the highest incorrect confidence (hic) scores assigned to each of 10,000 perturbed inputs. These scores are normally distributed.

hic score that exceeds a given δ , say 0.6. For data distributed normally, as in this case, we begin by calculating the *statistical standard score (Z-Score)*, which is the number of standard deviations by which the value of a raw score (in our case, δ) exceeds the mean value. Once the Z-score is obtained, we can use the normal distribution function, which computes the correct probability of the event using the Gaussian function. In our case, we get $\text{hic}(\vec{x}) \sim \mathcal{N}(\mu = 0.499, \Sigma = 0.059^2)$, where μ is the average score and Σ is the variance. The resulting Z-score is $\frac{\delta - \mu}{\sigma} = \frac{0.6 - 0.499}{0.059} = 1.741$, where σ is the standard deviation. Recall that our goal is to compute the plr score, which is the probability of the hic value not exceeding δ ; and so we obtain that:

$$\begin{aligned} \text{plr}_{0.6,0.04}(N, \vec{x}_0) &= \text{NormalDistribution}(\text{Z-score}) \\ &= \text{NormalDistribution}(1.741) \\ &= \frac{1}{\sqrt{2\pi}} \int_{-\infty}^{t=1.741} e^{-\frac{t^2}{2}} dt \\ &= 0.9591 \end{aligned}$$

We thus arrive at a probabilistic local robustness score of 95.91%. Consequently, a perturbed image drawn uniformly at random has a chance of $(1 - 0.9591) = 4.08\%$ of constituting an adversarial input.

Of course, given data obtained empirically, as in our case, we need a reliable way to determine whether the data is distributed normally before applying the aforementioned approach. A *goodness-of-fit* test is a procedure for determining whether a set of n samples can be considered as drawn from a specified distribution. A common goodness-of-fit test for the normal distribution is the Anderson-Darlin test (Anderson, 2011), which is used by widespread statistical, commercial applications such as SPSS (IBM, 2001) and JMP (SAS, 2001). Usually, a few hundred samples are more than enough to determine that a distribution is normal via the Anderson-Darlin test.

3.3. The Box-Cox Transformation

Unfortunately, most often the hic values of the perturbed inputs around \vec{x}_0 are not normally distributed, and so the aforementioned approach does not immediately apply. For example, in our VGG16-10 model, out of the 10,000 points (images) in the CIFAR10’s test set, only 1282 (less than 13%) points demonstrated normally-distributed hic values for the perturbed inputs around them (as determined by the Anderson-Darlin test). Figure 2 illustrates the abnormal distribution of hic values of perturbed input around one of the other input points, where we consequently cannot use the normal distribution function to estimate the probability of adversarial inputs in the population.

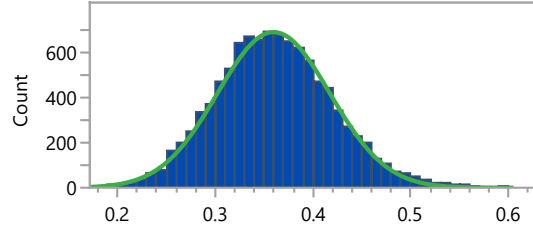


Figure 2. A histogram depicting the highest incorrect confidence (hic) scores of each of 10,000 perturbed inputs around one of the test points. This time, these scores are *not* normally distributed.

The strategy that we propose for handling abnormal distributions of data like the one depicted in Figure 2 is to apply *statistical transformations*. Such transformations preserve key properties of the data, while producing a normally distributed measurement scale (Griffith et al., 2013) — effectively converting the given distribution into a normal one. Power transformations are widely used by statisticians, and supported by standard statistical applications such as SPSS and JMP. There are two main transformations used to normalize probability distributions: Box-Cox (Box & Cox, 1982) and Yeo-Johnson (Yeo & Johnson, 2000). Here, we focus on the Box-Cox power transformation, which is preferred for distributions of positive hic values (as in our case). Box-Cox is a continuous, piecewise-linear power transform function, parameterized by a real-valued λ , defined as follows:

Definition 3.2. The Box-Cox_λ power transformation of input x is:

$$\lambda(x) = \begin{cases} \frac{x^\lambda - 1}{\lambda} & \text{if } \lambda \neq 0 \\ \ln(x) & \text{if } \lambda = 0 \end{cases}$$

The selection of the λ value is crucial for the successful normalization of the data. There are multiple automated methods for λ selection, which go beyond our scope here (Rossi, 2018; Asar et al., 2017). For our implementation of the technique, we used the common *SciPy* Python package (SciPy, 2021), which implements one of these automated methods.

Figure 3 depicts the distribution of the data from Figure 2, after applying the Box-Cox transformation, with an automatically calculated $\lambda = 0.534$ value. As the figure shows, the data is now normally distributed: $\text{hic}(\vec{x}) \sim \mathcal{N}(\mu = -0.79, \Sigma = 0.092^2)$. The normal distribution was confirmed with the Anderson-Darlin test, with a confidence score of over 99%. Following the Box-Cox transformation, we can now calculate the Z-Score, which gives 3.71, and the corresponding plr score, which turns out to be 99.98%—a high score of robustness for this image from the test set.

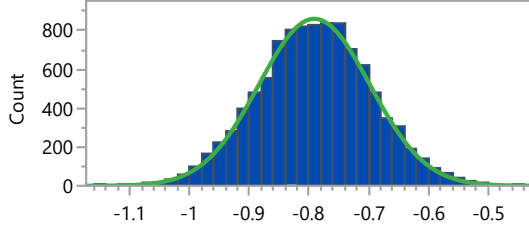


Figure 3. A histogram depicting the highest incorrect confidence (hic) scores of each of the 10,000 perturbed images from Figure 2, after applying the Box-Cox transformation.

3.4. The RoMA Certification Algorithm

Based on the previous sections, our algorithm for computing plr scores is given as Algorithm 1.

Algorithm 1 Compute Probabilistic Local Robustness($\delta, \epsilon, \vec{x}_0, n, N, \mathcal{D}$)

```

1: for  $i := 1$  to  $n$  do
2:    $x^i = \text{CreatePerturbedPoint}(\vec{x}_0, \epsilon, \mathcal{D})$ 
3:    $\text{hic}[i] \leftarrow \text{Predict}(N, x^i)$ 
4: end for
5: if Anderson-Darlin(hic  $\neq$  NORMAL) then
6:   hic  $\leftarrow$  Box-Cox(hic)
7:   if Anderson-Darlin(hic  $\neq$  NORMAL) then
8:     Return "Fail"
9:   end if
10: end if
11: avg  $\leftarrow$  Average(hic)
12: std  $\leftarrow$  StdDev(hic)
13: z-score  $\leftarrow$  Z-Score(avg, std,  $\delta$ )
14: Return NormalDistribution(z-score)
    
```

The inputs to the algorithm are: (i) δ , the confidence threshold for a distinctly adversarial input; (ii) ϵ , the maximum amplitude of perturbation that can be added to \vec{x}_0 ; (iii) \vec{x}_0 , the input point whose plr score is being computed; (iv) n , the number of perturbed samples to generate around \vec{x}_0 ; (v) N , the neural network; and (vi) \mathcal{D} , the distribution from which adversarial inputs are drawn.

The algorithm starts by generating n perturbed inputs around

the provided \vec{x}_0 , each drawn according to the provided distribution \mathcal{D} and with a perturbation that does not exceed ϵ (lines 1–2). Line 3 then stores the hic score of each perturbed input in the *hic* array. Next, lines 5–10 confirm that the samples’ hic values distribute normally, optionally applying the Box-Cox transformation if needed. Finally, on lines 11–13, the algorithm calculates the probability of randomly perturbing the input into a distinctly adversarial input using the properties of the normal distribution, and returns the computed $\text{plr}_{\delta, \epsilon}(N, \vec{x}_0)$ score on line 14.

Soundness and Completeness. Algorithm 1 depends on the distribution of $\text{hic}(\vec{x})$ being normal. If the distribution is initially not normal, the algorithm attempts to normalize it using the Box-Cox transformation. The Anderson-Darlin goodness-of-fit tests ensure that the algorithm will not treat an abnormal distribution as a normal one, and thus guarantee the soundness of the computed plr scores.

The algorithm’s completeness depends on its ability to always obtain a normal distribution. As our evaluation demonstrates, the Box-Cox transformation can indeed lead to a normal distribution very often. However, the transformation might fail in producing a normal distribution; this failure will be identified by the Anderson-Darlin test, and our algorithm will stop with a failure notice in such cases. In that sense, Algorithm 1 is incomplete. In practice, failure notices by the algorithm can sometimes be circumvented — by increasing the sample size, or by evaluating the robustness of other input points.

In our evaluation, we observed that the success of Box-Cox often depends on the value of ϵ . An analysis of the results indicated that small or large ϵ values more often led to failures, whereas mid-range values more often led to success. We speculate that small values of ϵ , which allow only tiny perturbation to the input, cause the model to assign similar hic values to all points in the ϵ -ball, resulting in a small variety of hic values for all sampled points; and consequently, the distribution of hic values is nearly uniform, and is impossible to normalize. We further speculate for large values of ϵ , where the corresponding ϵ -ball contains a significant chunk of the input space, the sampling produces a close-to-uniform distribution of all possible labels, and consequently a close-to-uniform distribution of hic values, which is impossible to normalize. We thus argue that the mid-range values of ϵ are the more relevant ones. Adding better support for cases where Box-Cox fails, for example by using additional statistical transformations and providing informative output to the user, remains a work in progress.

4. Evaluation

For evaluation purposes, we implemented Algorithm 1 as a proof-of-concept tool. The tool is written in Python 3.7.10,

uses the TensorFlow 2.5 and Keras 2.4 frameworks. For our models, we used Resnet-10, Resnet-100, VGG16-10, VGG16-200, and Densenet, as described in Table 1, all trained using the CIFAR10 data set. All experiments mentioned in the following section were run using the *Google Colab Pro* environment, with an NVIDIA-SMI 470.74 GPU and a single-core Intel(R) Xeon(R) CPU @ 2.20GHz. The code for the tool, the experiments, and the model’s training is (anonymously) available online ([Anonymized, 2021](#)), and will be publicly released with the final version of this paper.

Table 1. Neural network models’ properties.

Name	Base Model	# Epochs	Accuracy	Loss
Resnet-10	Resnet	10	0.72	1.07
Resnet-100	Resnet	100	0.91	0.4456
VGG16-10	VGG16	10	0.73	0.8329
VGG16-200	VGG16	200	0.76	2.7082
Densenet	Densenet	200	0.93	0.5335

4.1. Experiment 1: Measuring the sensitivity of robustness to perturbation size

By our notion of robustness given in Definition 3.1, it is likely that the $plr_{\delta,\epsilon}(N, \vec{x}_0)$ score decreases as ϵ increases. For our first experiment, we set out to measure the rate of robustness decrease. Using our Densenet model, we repeatedly invoked Algorithm 1 to compute plr scores for increasing values of ϵ . For our \vec{x}_0 , we arbitrarily selected the first 200 images from the CIFAR10 test set, and measured the average robustness of the images for each ϵ . The averaged results (depicted in Figure 4) indicates a correlation between ϵ and the robustness score. This result is supported by earlier findings ([Webb et al., 2018](#)).

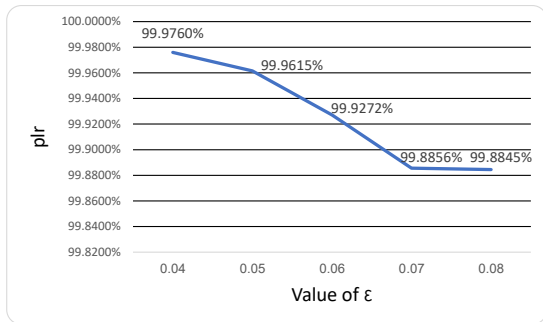


Figure 4. Average plr score of the first 200 images from CIFAR10 dataset, computed on our VGG16-10 model as a function of ϵ .

The experiment was conducted by running Algorithm 1 with $\delta = 0.6$, $n = 1,000$, $N =$ Densenet on each of the first 200 input images from the CIFAR10 test set. Running the

algorithm took less than 20 minutes for the entire experiment. We note here that Algorithm 1 naturally lends itself to parallelization, as each perturbed input can be evaluated independently of the others; we leave adding these capabilities to our proof-of-concept implementation for future work.

4.2. Experiment 2: Comparing robustness across models

The ability to efficiently compute plr scores allows us to compare multiple models based on their robustness. Using Algorithm 1, we computed the plr scores for each of our five models from table 1, averaged over the first 200 images from the CIFAR10 test set. We arbitrarily set $\epsilon = 0.04$, $n = 1,000$ and $\delta = 0.6$. The average plr scores appear in Figure 5, and indicate that, per base model, a higher number of epochs leads to a higher robustness score.

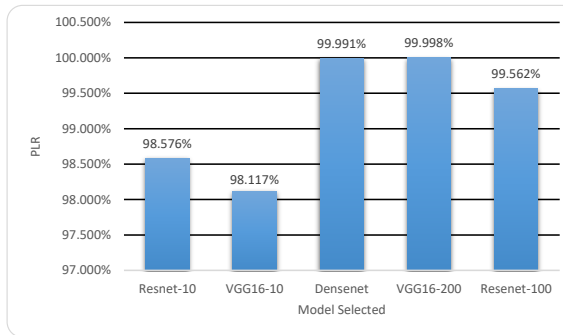


Figure 5. A comparison of average plr scores, computed over the first 200 CIFAR10 images, among the models appearing in Table 1.

Running Algorithm 1 as part of the described experiment with 1,000 perturbation samples for each image required less than seven minutes for the entire experiment.

Completeness Rates. We observed that the completeness rate (the number of samples for which Algorithm 1 was successful, divided by the total number of samples) varies between the models: in VGG16-10 and VGG-200, the completeness rates were 88% and 75.5% respectively; in Resnet-10 and Resnet-100 the rates were 82.5% and 86.5% respectively; and in Densenet, the rate was 78%. To improve these rates, the steps described in Section 3.4 can be applied.

4.3. Experiment 3: Categorical robustness

For our final experiment, we focused on *categorical robustness*, where we first measure the robustness of inputs labeled as a specific category, and then compare the robustness scores across categories.

We ran Algorithm 1 on our $N =$ VGG16-10 model, with $\delta =$

0.6, $\epsilon = 0.04$, and $n = 1,000$ for all 10,000 CIFAR10 test set images. The results, separated by category, appear in Table 2. For each category we list the average plr score, the standard deviation of the data which indicates the scattering for each category, and the probability of randomly generating an adversarial input (the “Adv” column, calculated as $1 - \text{plr}$).

Table 2. An analysis of average, per-category robustness, computed over all 10,000 images from the CIFAR10 dataset.

Category	plr	Std-Dev.	Adv
Airplane	99.143%	5.18%	0.857%
Automotive	99.372%	3.86%	0.628%
Bird	97.226%	8.87%	2.774%
Cat	97.112%	8.77%	2.888%
Deer	98.586%	6.25%	1.414%
Dog	97.233%	8.58%	2.767%
Frog	98.524%	6.39%	1.476%
Horse	98.606%	6.09%	1.394%
Ship	98.389%	6.63%	1.611%
Truck	99.390%	4.26%	06.10%

The results expose an interesting insight, namely the high variability in robustness between the different categories. For example, the probability of encountering an adversarial input for inputs classified as Cats is four times greater than the probability of encountering an adversarial input for inputs classified as Trucks. We observe that the standard deviation for these two categories is very small, which indicates that they are “far apart” — the difference between Cats and Trucks, as determined by the network, is generally greater than the difference between two Cats or between two Trucks. We applied a *T-test* and a *binomial test*, which are well-established statistical tools for measuring the difference between two sets of values, to the Cat and Truck categories. The tests produced a similarity score of less than 0.1%, indicating that the two categories are indeed distinctly different. The important conclusion that we can draw is that the per-category robustness of models can be far from uniform.

It is common in certification methodology to assign each sub-system a different robustness objective score depending on the sub-system’s criticality (Federal Aviation Administration, 1993). Yet, to the best of our knowledge, this is the first time such differences in neural networks’ categorial robustness have been measured and reported. We believe categorial robustness could affect DNN certification efforts, by allowing engineers to require separate robustness thresholds for different categories. For example, for a traffic sign recognition DNN, a user might require a high robustness score for the “stop sign” category, and be willing to settle

for a lower robustness score for the “parking sign” category.

Running Algorithm 1 on the entire CIFAR10 test set (10,000 samples) took 37 minutes. The completeness rate for the experiment was 90.48%.

5. Summary and Discussion

5.1. Summary

In this paper, we introduced RoMA — a novel statistical and scalable method for measuring the probabilistic local robustness of a black-box, high-scale DNN model. We demonstrated RoMA’s applicability in several aspects and on multiple common DNN models. The key advantages of RoMA over existing methods are: (i) it uses straightforward and intuitive statistical method for measuring DNN robustness; (ii) it is scalable; (iii) it works on black-box DNN models and makes no assumptions such as Lipschitz continuity or piecewise-linear constraints; and (iv) the method is quick in comparison to formal verification methods and other methods that require hours or more for analyzing local robustness (Wang et al., 2018). Our approach’s limitation stems from the dependence on the normal distribution of the perturbed inputs, and will fail whenever the Box-Cox transformation does not normalize the perturbed input distribution.

The plr scores computed by RoMA indicate the risk of using a DNN model, and can allow regulatory agencies to conduct *risk mitigation* procedures: a common practice for integrating sub-systems with a known MTBF into safety-critical systems. The ability to perform risk and robustness assessment is an important step towards using DNN models in the world of safety-critical applications, such as medical devices, UAVs, automotive, and others. We believe that our work also showcases the potential key role of *categorial robustness* in this endeavor.

Moving forward, we intend to: (i) evaluate our tool on additional norms, beyond L_∞ ; and (ii) better characterize the cases where the Box-Cox transformation fails, and search for other statistical tools can succeed in those cases; and (iii) improves the scalability of our tool by adding parallelization capabilities.

References

Amir, G., Wu, H., Barrett, C., and Katz, G. An SMT-Based Approach for Verifying Binarized Neural Networks. In *Proc. 27th Int. Conf. on Tools and Algorithms for the Construction and Analysis of Systems (TACAS)*, pp. 203–222, 2021.

Anderson, B. and Sojoudi, S. Data-Driven Assessment of Deep Neural Networks with Random Input Uncertainty,

2020. Technical Report. <http://arxiv.org/abs/2010.01171>.
- Anderson, T. Anderson-Darling Tests of Goodness-of-Fit. *Int. Encyclopedia of Statistical Science*, 1:52–54, 2011.
- Anonymized. RoMA: Code and Experiments, 2021. <https://drive.google.com/drive/folders/1rIrLIwiwDCsueJUMGMzcQfxqWwP7g18y?usp=sharing>.
- Asar, Ö., Ilk, O., and Dag, O. Estimating Box-Cox Power Transformation Parameter Via Goodness-of-Fit Tests. *Communications in Statistics-Simulation and Computation*, 46(1):91–105, 2017.
- Author, N. N. Suppressed for anonymity, 2021.
- Bastani, O., Ioannou, Y., Lampropoulos, L., Vytiniotis, D., Nori, A., and Criminisi, A. Measuring Neural Net Robustness with Constraints. In *Proc. 30th Conf. on Neural Information Processing Systems (NIPS)*, 2016.
- Box, G. and Cox, D. An Analysis of Transformations Revisited, Rebutted. *Journal of the American Statistical Association*, 77(377):209–210, 1982.
- Carlini, N. and Wagner, D. Towards Evaluating the Robustness of Neural Networks. In *Proc. 2017 IEEE Symposium on Security and Privacy (S&P)*, pp. 39–57, 2017.
- Cohen, J., Rosenfeld, E., and Kolter, Z. Certified adversarial robustness via randomized smoothing. In *International Conference on Machine Learning*, pp. 1310–1320. PMLR, 2019.
- Dmitriev, K., Schumann, J., and Holzapfel, F. Toward certification of machine-learning systems for low criticality airborne applications. In *2021 IEEE/AIAA 40th Digital Avionics Systems Conference (DASC)*, pp. 1–7. IEEE, 2021.
- Duda, R. O., Hart, P. E., and Stork, D. G. *Pattern Classification*. John Wiley and Sons, 2nd edition, 2000.
- Dvijotham, K., Garnelo, M., Fawzi, A., and Kohli, P. Verification of Deep Probabilistic Models, 2018. Technical Report. <http://arxiv.org/abs/1812.02795>.
- European Union Aviation Safety Agency. Artificial Intelligence Roadmap: A Human-Centric Approach To AI In Aviation, 2020. <https://www.easa.europa.eu/newsroom-and-events/news/easa-artificial-intelligence-roadmap-10-published>.
- FAA. System Safety Handbook, 2021a. https://www.faa.gov/regulations_policies/handbooks_manuals/aviation/risk_management/ss_handbook/.
- FAA. System Safety Handbook, 2021b. https://www.faa.gov/documentLibrary/media/Advisory_Circular/AC-23-1309-1E.pdf.
- Federal Aviation Administration. RTCA, Inc., Document RTCA/DO-178B , 1993. <https://nla.gov.au/nla.cat-vn4510326>.
- Goodfellow, I., Shlens, J., and Szegedy, C. Explaining and Harnessing Adversarial Examples, 2014. Technical Report. <http://arxiv.org/abs/1412.6572>.
- Griffith, D. A., Amrhein, C., and Huriot, J.-M. *Econometric advances in spatial modelling and methodology: essays in honour of Jean Paelinck*, volume 35. Springer Science & Business Media, 2013.
- Hammersley, J. *Monte Carlo Methods*. Springer Science & Business Media, 2013.
- He, K., Zhang, X., Ren, S., and Sun, J. Deep Residual Learning for Image Recognition. In *Proc. 29th IEEE Conf. on Computer Vision and Pattern Recognition (CVPR)*, pp. 770–778, 2016.
- Huang, C., Hu, Z., Huang, X., and Pei, K. Statistical Certification of Acceptable Robustness for Neural Networks. In *Proc. Int. Conf. on Artificial Neural Networks (ICANN)*, pp. 79–90, 2021.
- Huang, G., Liu, Z., Van Der Maaten, L., and Weinberger, K. Densely Connected Convolutional Networks. In *Proc. 30th IEEE Conf. on Computer Vision and Pattern Recognition (CVPR)*, pp. 2261–2269, 2017a.
- Huang, X., Kwiatkowska, M., Wang, S., and Wu, M. Safety Verification of Deep Neural Networks. In *Proc. 29th Int. Conf. on Computer Aided Verification (CAV)*, pp. 3–29, 2017b.
- IBM. IBM SPSS Website, 2001. <https://www.ibm.com/products/spss-statistics>.
- Ilyas, A., Santurkar, S., Tsipras, D., Engstrom, L., Tran, B., and Madry, A. Adversarial Examples are not Bugs, they are Features, 2019. Technical Report. <http://arxiv.org/abs/1905.02175>.
- Jacoby, Y., Barrett, C., and Katz, G. Verifying Recurrent Neural Networks using Invariant Inference. In *Proc. 18th Int. Symposium on Automated Technology for Verification and Analysis (ATVA)*, pp. 57–74, 2020.

- Katz, G., Barrett, C., Dill, D., Julian, K., and Kochenderfer, M. Reluplex: An Efficient SMT Solver for Verifying Deep Neural Networks. In *Proc. 29th Int. Conf. on Computer Aided Verification (CAV)*, pp. 97–117, 2017.
- Katz, G., Barrett, C., Dill, D., Julian, K., and Kochenderfer, M. Reluplex: a Calculus for Reasoning about Deep Neural Networks. *Formal Methods in System Design (FMSD)*, 2021.
- Kearns, M. J. *Computational Complexity of Machine Learning*. PhD thesis, Department of Computer Science, Harvard University, 1989.
- Krizhevsky, A. and Hinton, G. Learning Multiple Layers of Features from Tiny Images, 2009. Technical Report.
- Langley, P. Crafting papers on machine learning. In Langley, P. (ed.), *Proceedings of the 17th International Conference on Machine Learning (ICML 2000)*, pp. 1207–1216, Stanford, CA, 2000. Morgan Kaufmann.
- Mangal, R., Nori, A., and Orso, A. Robustness of Neural Networks: A Probabilistic and Practical Approach. In *Proc. 41st IEEE/ACM Int. Conf. on Software Engineering: New Ideas and Emerging Results (ICSE-NIER)*, pp. 93–96, 2019.
- Michalski, R. S., Carbonell, J. G., and Mitchell, T. M. (eds.). *Machine Learning: An Artificial Intelligence Approach, Vol. I*. Tioga, Palo Alto, CA, 1983.
- Mitchell, T. M. The need for biases in learning generalizations. Technical report, Computer Science Department, Rutgers University, New Brunswick, MA, 1980.
- Newell, A. and Rosenbloom, P. S. Mechanisms of skill acquisition and the law of practice. In Anderson, J. R. (ed.), *Cognitive Skills and Their Acquisition*, chapter 1, pp. 1–51. Lawrence Erlbaum Associates, Inc., Hillsdale, NJ, 1981.
- Pereira, A. and Thomas, C. Challenges of Machine Learning Applied to Safety-Critical Cyber-Physical Systems. *Machine Learning and Knowledge Extraction*, 2(4):579–602, 2020.
- Rossi, R. *Mathematical Statistics: an Introduction to Likelihood Based Inference*. John Wiley & Sons, 2018.
- Samuel, A. L. Some studies in machine learning using the game of checkers. *IBM Journal of Research and Development*, 3(3):211–229, 1959.
- SAS. Sas jmp website, 2001. url<https://www.ibm.com/products/spss-statistics>.
- Scipy. Scipy Python package, 2021. <https://scipy.org/>.
- Simonyan, K. and Zisserman, A. Very Deep Convolutional Networks for Large-Scale Image Recognition. In *Proc. 3rd Int. Conf. on Learning Representations (ICLR)*, pp. 1–14, 2015.
- Taherdoost, H. Sampling methods in research methodology; how to choose a sampling technique for research. *How to Choose a Sampling Technique for Research (April 10, 2016)*, 2016.
- Vidot, G., Gabreau, C., Ober, I., and Ober, I. Certification of Embedded Systems Based on Machine Learning: A Survey, 2021. Technical Report. <http://arxiv.org/abs/2106.07221>.
- Wang, S., Pei, K., Whitehouse, J., Yang, J., and Jana, S. Formal Security Analysis of Neural Networks using Symbolic Intervals. In *Proc. 27th USENIX Security Symposium*, pp. 1599–1614, 2018.
- Webb, S., Rainforth, T., Teh, Y., and Pawan Kumar, M. A Statistical Approach to Assessing Neural Network Robustness, 2018. Technical Report. <http://arxiv.org/abs/1811.07209>.
- Weng, L., Chen, P.-Y., Nguyen, L., Squillante, M., Boopathy, A., Oseledets, I., and Daniel, L. PROVEN: Verifying Robustness of Neural Networks with a Probabilistic Approach. In *Proc. 36th Int. Conf. on Machine Learning (ICML)*, pp. 6727–6736, 2019.
- Wu, H., Ozdemir, A., Zeljić, A., Irfan, A., Julian, K., Gopinath, D., Fouladi, S., Katz, G., Păsăreanu, C., and Barrett, C. Parallelization Techniques for Verifying Neural Networks. In *Proc. 20th Int. Conf. on Formal Methods in Computer-Aided Design (FMCAD)*, pp. 128–137, 2020.
- Yeo, I.-K. and Johnson, R. A New Family of Power Transformations to Improve Normality or Symmetry. *Biometrika*, 87(4):954–959, 2000.